Petroleum 10 (2024) 135–149

Contents lists available at ScienceDirect

Petroleum

journal homepage: www.keaipublishing.com/en/journals/petlm

Full Length Article

Auto-tuning PVT data using multi-objective optimization: Application of NSGA-II algorithm

Abdolhadi Zarifi [a, c], Mohammad Madani [a, b, c, *], Mohammad Jafarzadegan [a]

[a] Reservoir Engineering Systems, Petroleum Engineering Department, Main Office Building of National Iranian South Oil Company (NISOC), Ahvaz, Iran
[b] Reservoir Engineering Division, Petroleum Engineering Department, Petroleum Engineering and Development Company (PEDEC), Tehran, Iran
[c] Combined Planning Management, National Iranian Oil Company (NIOC), Tehran, Iran

ARTICLE INFO

Article history:
Received 22 July 2022
Received in revised form
14 October 2022
Accepted 17 April 2023

Keywords:
Auto-tuning
PVT
Equation of state
NSGA-II
Multi-objective optimization

ABSTRACT

Reservoir simulation is known as perhaps the most widely used, accurate, and reliable method for field development in the petroleum industry. An integral part of a reliable reservoir simulation process is to consider robust and rigorous tuned EOS models. Traditionally, EOS models are tuned iteratively through arduous workflows against experimental PVT data. However, this comes with a number of drawbacks such as forcingly using weight factors, which upon alteration adversely affects the optimization process. The objective of the current work is thus to introduce an auto-tune PVT matching tool using NSGA-II multi-objective optimization. In order to illustrate the robustness of the presented technique, three different PVT samples are used, including two black-oil and one gas condensate sample. We utilize Peng-Robinson EOS during all the manual and auto-tuning processes. Comparison of auto-tuned EOS-generated results with those of experimental and computed statistical error values for these samples clearly show that the proposed method is robust. In addition, the proposed method, contrary to the manual matching process, provides the engineer with several matched solutions, which allows them to select a match based on the engineering background to be best amenable to the problem at hand. In addition, the proposed technique is fast, and can output several solutions within less time compared to the traditional manual matching method.

1. Introduction

The process of reservoir fluid characterization is of paramount importance to production processes, designing facilities, and optimization [1,2]. The constituents of reservoir fluids encompass myriad natural hydrocarbon and non-hydrocarbon substances, with hydrocarbon molecules ranging from simple methane to molecules that might possess a hundred carbon atoms. Hydrocarbon reservoir fluids are inherently complicated from the standpoint of chemistry science. In addition, precise prediction of parameters such as oil-in-place and oil recovery with time is a major topic of concern to national oil companies worldwide. Inaccurate and unreliable fluid characterization along with unintentionally large magnitude of uncertainties adversely affect the estimation of such parameters. Moreover, experimental-based techniques are both expensive, and time-consuming. The reservoir engineers are, therefore, encouraged to utilize robust modeling techniques such as equation of state (EOS) for the purpose of prediction of hydrocarbon fluid phase behavior [3,4].

Despite the fact that underground naturally-occurring hydrocarbon fluids are characteristically complex, the literature substantiates that equation of states are rigorously capable of modeling phase behavior for such complex fluids. Equations of state have been used to model fluid and predict the thermodynamic state of the system which encompass fluid models in production engineering to highly complex models used in compositional reservoir simulation, enhanced oil recovery (EOR) processes such as miscible gas injection and chemical/thermal EOR methods [5–7]. Various EOSs have been proposed by many researchers [8], and the

* Corresponding author.
E-mail address: m_madani70@yahoo.com (M. Madani).
Peer review under responsibility of Southwest Petroleum University.

Production and Hosting by Elsevier on behalf of KeAi

https://doi.org/10.1016/j.petlm.2023.04.003

development dates back to 1949 when Redlich and Kwong (RK) [9] designed a two-parameter cubic EOS. Since then, several researchers attempted to enhance the initial RK EOS form. Aside from RK based equation of states, two other prominent cubic EOSs include Soave-Redlich-Kwong (SRK) [10] and Peng-Robinson (PR) [11]. It is worthwhile mentioning that in spite of reportedly existing several modified forms of RK EOS in the open literature, only SRK and PR are widely used and accepted for hydrocarbon systems and their mixtures.

In order to attain a sensible match between EOS model results and experimental data, trial-and-error manual adjustments to EOS parameters are customary in the petroleum industry, and the regression variables are essentially a desired number of EOS parameters in this regard [12]. For this purpose, disparate regression variables have been proposed by researchers, using which one can manually tune an EOS [13–17]. Coats and Smart [18] put forth heavy fractions-methane binary interaction coefficients, and omega A and B of methane/heavy fractions as tuning parameters. Christensen [19] asserted a three-parameter tuning approach which includes volume translation factor as well as the most two sensitive factors amongst T_c, P_c, and Omega for C_{7+}. Whitson and Brule [20] enlarged Coats and Smart's tuning factors to possess molecular weight (M_w) and volume correction factor (C_i). Selection of nitrogen and carbon dioxide omega parameters, and C_{7+} properties such as molecular weight, critical pressure, and temperature as adjustable variables have also been proclaimed in the literature [8].

The calibration process of an EOS is generally an arduous task, and largely depends on the expert's experience. In fact, there exist a myriad of available regression parameters to choose from for the EOS tuning process, and one cannot certainly determine which sets of regression parameters are the most sensible to select. Favorable match results are routinely achieved through tedious iterative workflows, and various engineers face different outcomes since no certain robust method of selecting an equation of state, types and number of tuning parameters are found in the literature. To overcome these difficulties, search-based evolutionary algorithms have been proposed. For instance, Taghizadeh Sarvestani et al. [13] put forward a novel technique based on genetic algorithm (GA) to obtain the most suitable regression variables to match the EOS model with experimental data. Zarifi and Daryasafar [8] proposed a precise and simple generalized auto-tune methodology based on Monte-Carlo and genetic algorithm to find the best match between the experimental data and EOS. However, the proposed techniques suffer from three major deficiencies: (1) each regression parameter should be assigned a weight factor, which upon alteration adversely affects the optimization process; (2) the number of data points measured in a particular PVT (pressure-volume-temperature) experiment impacts the objective function and tuning process; and (3) the tuning process only leads to one converged tuned EOS and, thus, cannot represent the optimized match of simultaneous PVT properties.

The main objective of the current study is therefore to introduce a methodology immune from the aforementioned issues. In this study, hence, a multi-objective optimization methodology is applied to auto-tune EOS based on non-dominated sorting genetic algorithm (NSGA-II). Multi-objective optimization techniques make it possible to obtain a series of tuned EOS, each of which having advantages over the others, and engineers can select the most suitable tuned EOS to meet their requirements. The reliability of the aforementioned methodology is implied using three fluid samples (two black-oil and one gas condensate sample) that are different in PVT properties. Notice that we will use PR EOS during all the manual and auto-tuning processes.

2. Background

2.1. Genetic algorithm (GA)

Genetic algorithms (GA) are stochastically search-based techniques focusing on natural selection mechanisms generally observed in biological genetics [21]. A preliminary set of random solutions embodied as “solution population” fulfilling problem constraints is utilized to commence GA [22]. During the progress, the obtained solutions are firstly ranked according to their performance with regard to objective function(s). Then, top ranked solutions are become subject to a subsequent number of genetic processes such as cross-over, and mutation to generate new solutions, followed by determination of best solutions. This iterative process is repeated while maintaining the best solutions of the foregoing generations. The ranking process of solutions are carried out using their individual fitness scores in a specific generation, and the best solutions are subsequently spirited away to next generation. It is reported that GA may converge to an optimum solution for some problems, though for others, it is less likely for GA to find all solutions which means that several isolated minima in the solution space might be missed out; in this situation, a number of highest performing solutions are selected when no enhanced solution is found during a period of runtime.

Several researchers have devoted their energy to shed light on solving engineering problems through GA [23–27]. Romero and Carter (2001) [28] made use of GA for the purpose of reservoir characterization. Velez-Lang (2005) [29] introduced several researches encompassing the deployment of GA in well log analysis, seismology, reservoir flow simulation, and hydraulic fracturing design. Zarifi et al. (2018) [8] made use of GA for the objective of auto-tuning black oil and gas condensate fluid samples.

2.2. Multi-objective optimization

Vector optimization, multi-criteria optimization or multi-objective optimization are all similar terms referring to techniques associated with obtaining decision variable vectors that honor the given constraints and objective functions [30,31]. In such problems, many cost functions or objectives (a vector of objectives) ought to be either maximized or minimized concurrently. There usually exists a contradictory behavior among these objectives in such a way that enhancing each might aggravate another. Hence, no single optimum solution can usually be found that would serve all objective functions in the best way simultaneously. Instead, a set of optimal solutions known as Pareto optimal solutions or simply “Pareto front” is prevalent in multi-objective optimization problems [32–36]. Pareto solutions refer to kind of solutions which are non-dominated to each other, while being superior to other solutions in the search space. Therefore, no likely single solution is found to be preferable over all other solutions regarding all objectives. Any change in the vector of design variables will exacerbate one objective at least [37]. Because of their naturally suited properties such as parallel or population-based search nature, evolutionary algorithms are vastly utilized for multi-objective optimization. In this regard, most defects prevalent in classical techniques are eradicated when dealing with solving multi-objective optimization problems. As an example, it is not required

for performing several runs to unearth Pareto front or quantify the significance of each objective with the aid of numerical weights.

2.3. Non-dominated sorted genetic algorithm II (NSGA-II)

The NSGA-II is a multi-objective, elitist, and fast GA which has been interestingly used in several engineering optimization problems, has received attention in myriad disciplines. NSGA-II is considered the most renowned multi-objective algorithm from the so-far developed evolutionary algorithms. This algorithm utilizes the GA operators as well as two population-sorting criteria: crowding distance and non-dominance [38,39]. NSGA-II acts as an optimization algorithm to obtain a set of pareto-optimal. The non-dominated fast sorting method is used to acquire a set of equally acceptable solutions which are the closest to pareto-optimal front; using the concept of crowding distance, the diversity of the pareto-optimal set is maintained; and both the offspring and parent populations participate through the concept of elitism, which improves the convergency rate of the optimization algorithm [39–42]. The NSGA-II procedure is shown in Fig. 1.

The main procedural parts of NSGA-II include.

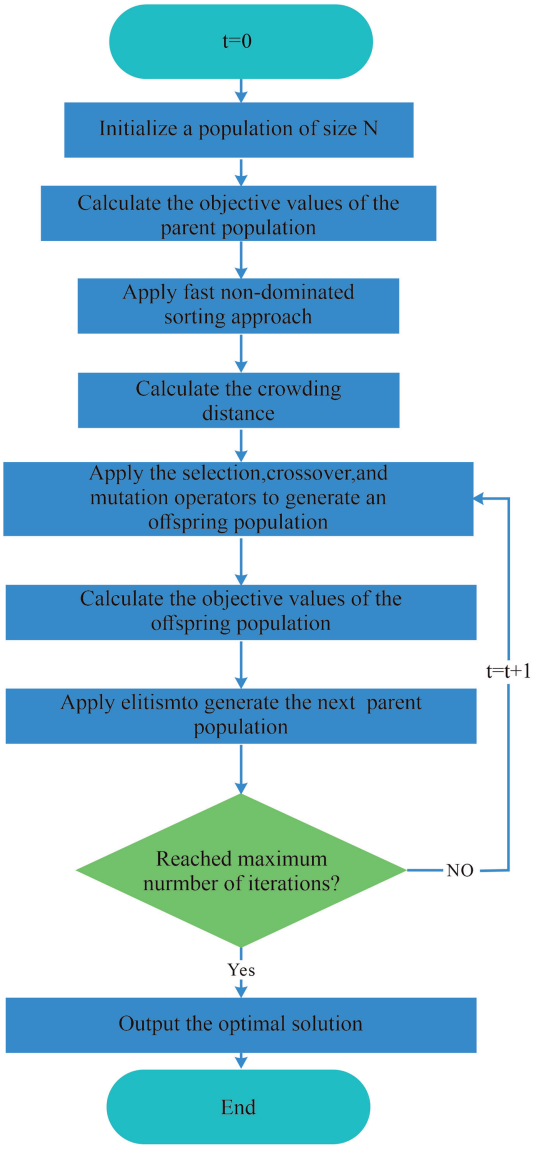

Fig. 1. NSGA-II procedure.

(a) Fast non-dominated sorting technique

Population H(t) is initially sorted into different non-dominated fronts. For any H*(t) ε H (t), if and only if H*(t) honors the following relationship:

$$\begin{aligned} &\neg\exists H_i(t)\neq H^*(t)(i=1,2,...,N)\in H(t)\\ &\forall j\in\{1,2,3\}\{E_j[H_i(t)]\le E_j[H^*(t)]\}\\ &\wedge\exists k\in\{1,2,3\}\{E_k[H_i(t)]<E_k[H^*(t)]\} \end{aligned} \quad (1)$$

then $H^*(t)$ may be called a non-dominated individual. Note that E denotes the objective function here. With $\boldsymbol{H}(t)$ being sorted via Eq. (1), all individuals in the first non-dominated front are obtained with their corresponding ranks being set to 1. The remaining individuals of $\boldsymbol{H}(t)$, except first ranked ones keep being sorted according to the above procedure. Then, the individuals existing in the second non-dominated front are selected with ranks equal to 2. This process keeps on until all fronts have been identified [39,42]. Fig. 2 attempts to illustrate fast non-dominated sorting approach in NSGA-II while dealing with two objective functions.

(b) Crowding distance operator

Now, individuals with the same rank are arranged in line with their objective values in ascending order. Note that the crowding distance of boundary individual is set equal to ∞. For the remaining individuals, the crowding distance is stated as [39,43]:

$$\delta_p(i)=\sum_{k=1}^{m}\frac{|E_k(i+1)-E_k(i-1)|}{E_k^{\max}-E_k^{\min}}, i\in\{2,3,...,n-1\} \quad (2)$$

where, p is the rank of the ith individual; n is the number of individuals whose ranks are p; $\delta_p(i)$ signifies the crowding distance of the ith individual; m is the number of the objective functions E_k denotes the kth objective function value; $E_k^{\max}$ and $E_k^{\min}$ denote the maximum and minimum values of the kth objective function, respectively.

(c) Selection operator

The binary tournament selection [39] is now applied to filter $\boldsymbol{H}(t)$ in accordance with crowding distance and the rank of each individual in $\boldsymbol{H}(t)$. Two individuals are randomly chosen from $\boldsymbol{H}(t)$ each time. When their ranks are the same, the individual with larger crowding distance will be selected; however, when their ranks are dissimilar, the individual with small rank will be chosen. Based on the abovementioned method, N individuals are selected to perform crossover operator.

(d) Crossover operator

Now the single-point and double-point crossover operation is performed with probability p_c for two randomly-selected individuals.

(e) Mutation operator

The reverse operation is conducted with probability p_m for each allele of each individual.

(f) Elitism operator

Elitism is the process of comparing offspring population with parent population, and then selecting the best N individuals as the

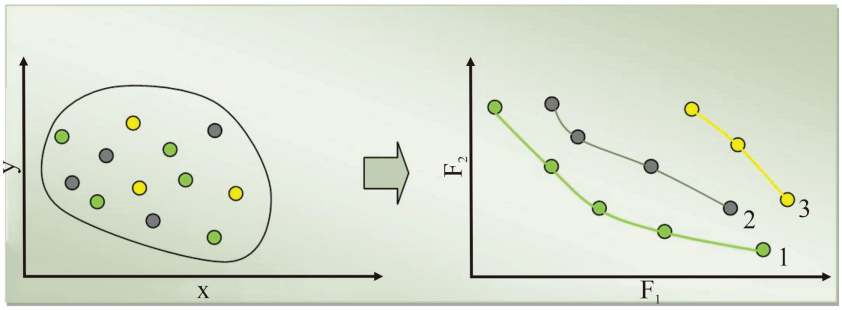

Fig. 2. Schematic illustration of non-dominated sorting method for two objective functions (i.e., F1 and F2) using NSGA-II algorithm.

next parent generation [42,44,45]. The elitism procedure may be given as:

(1) Offspring and parent populations are combined to create an impermanent generation of size 2 N;
(2) The temporary population is sorted using the fast non-dominated sorting method and then its crowding distance is estimated;
(3) The best N individuals are chosen as the subsequent parent generation. In the selection process, if two individuals have dissimilar ranks, the one with lesser rank is more appropriate; if two individuals possess the same rank, the one with larger crowding distance is more appropriate.

3. Methodology

The main objective of the present paper is to apply a new technique to tune EOS parameters while incorporating multi-objective non-sorted genetic algorithm instead of traditional single-objective algorithms. As mentioned, this technique ensures proper diversity of the generated populations, and further leads to a plausible match between EOS model results and experimental data. In addition, it allows us to choose a match based on the engineering background (i.e., how the tests were performed, and/or what the accuracy of the experimental data is from the fluid sample).

Given the complicated fluid properties calculations such as flash calculations, simulation of fluid tests (constant composition expansion, constant volume depletion, and differential liberation, etc.), we have made use of CMG WinProp [46] module as the main fluid properties calculating machine in this paper. In this sense, the initial population is generated via the random search. Note that each population represents an appropriate input data file in WinProp, with certain values for all tuning parameters. Based on the outputs generated from WinProp for each population, and using the optimization algorithm, producing next generations continue.

Generally speaking, the process of regressing EOS parameters using NSGA-II needs all the data required in conventional tuning of EOS. The required data includes fluid composition along with the initial components' properties, experimental data for different tests (oil and gas viscosity, oil formation volume factor, etc. all versus pressure) and regression parameters. It is worth mentioning that EOS type can also be taken into account as the regression parameter. Given the fact that WinProp supports 4 EOSs of Peng-Robinson, Peng-Robinson, SRK, and SRK (G&D), the introduced algorithm can apply each of these EOS for the purpose of regression process.

Having specified input and regression parameters, the algorithm automatically identifies the regression parameters, and attempts to generate values for the tuning parameters based upon random search and the defined boundary for each tuning parameter. This process is reiterated for the exact number of initial populations to generate new populations by means of revised values of tuning parameters. In order to conduct the optimization process, WinProp output results for different fluid properties which are called objective functions, are acquired in a sense that at the end of initialization process with n populations, m*n number of objective functions will prevail. The objective functions are estimated via the following formula:

$$OF_i = \sum_{j=1}^{m} \frac{\left| prop_{ij}^{\exp} - prop_{ij}^{EOS} \right|}{prop_{ij}^{\exp}} \quad i = 1 \ \ to \ \ n \tag{3}$$

In which OF_i represents the value of objective function for each PVT property (e.g., solution gas, formation volume factor, etc.), n is the total number of PVT properties measured experimentally, m is the number of experimental points for each PVT property, and superscripts exp and EOS indicate experimental value and EOS-generated result, respectively.

After determining the objective functions, the members of initial population are assigned different specific fronts based on the non-sorted method. Then, the existing members in each front are prioritized according to their crowding distance. In order to produce the next generation, dissimilar couples from the current population are selected according to crossover function. In this selection, the member with lower front and larger crowding distance takes higher priority to be elected. After the couples are successfully specified, the mutation and crossover functions take effect to produce new population (representing the new input data files to WinProp). By running these new populations which encompass new values for the regression parameters with the aid of WinProp, and further acquiring the output results, their objective functions values are accordingly estimated. Subsequently, using the pareto function and the method described previously, the generated and initial population are mixed and then ranked. Next population is selected according to rank and crowding distance. This process is iterated to the number of specified generations, ultimately leading to a set of solutions from which the engineer can choose based on his/her need and own sense of engineering. Fig. 3 depicts how NSGA-II multi-objective optimization algorithm is employed for auto-tuning PVT data.

4. Description of fluid samples

In this paper, we aim to show the application of non-sorted genetic algorithm customized for tuning EOS parameteres. To do that, a graphical user interface software package has also been developed which can help the engineer to perform EOS tuning in a feasible and more efficient manner. To check the validity, three fluid

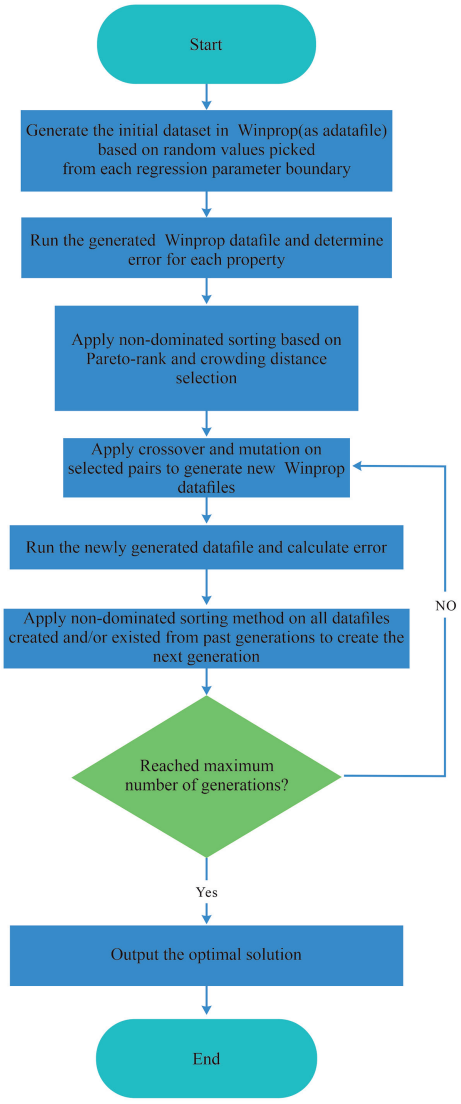

Fig. 3. Schematic representation of auto-tuning PVT data using NSGA-II multi-optimization algorithm.

samples with different compositions and different PVT behavior (two black oil and one gas condensate PVT samples) have been selected.

The first black oil sample (henceforth, named MB) is characterized in Table 1. Two different laboratory tests, a CCE test at the temperature of 164°F and one differential liberation test at 185°F are utilized to quantify fluid properties. Reported data encompass saturation pressure and relative oil volume in CCE (constant composition expansion) test at 164°F, and gas oil ratio, oil formation volume factor, liquid specific gravity and gas compressibility Z factor in differential liberation experiment at 164°F. These data are presented in Tables 2 and 3.

To explore the validity of the algorithm on diverse test results at different temperature, another black oil sample entitled MI is taken into account as well. Sample compositional data is shown in Table 4. Two CCE result data at two different temperatures of 110°F and 225°F shown in Tables 5 and 6 have been utilized for bubble point pressure and relative total volume. Differential liberation test results at 225°F which is used for characterizing seperated phase properties during pressure deplition, are presented in Table 7. Gas viscosity data has also been added to differential liberation results for further optimization.

Table 1
Fluid composition of sample MB.

Component	Mole fraction
N_2	0.001
CO_2	0.001
H_2S	0.000
C_1	0.312
C_2	0.055
C_3	0.061
IC_4	0.011
NC_4	0.032
IC_5	0.016
NC_5	0.018
FC_6	0.032
C_7–C_{13}	0.227
C_{14}–C_{21}	0.126
C_{22+}	0.108

The gas condensate sample (henceforth, named sample MA) is characterized in Table 8. Two different experiments have been designed to clarify this fluid behavior: CCE test to determine saturation pressure and relative oil voulme and CVD (constant volume deplition) test for obtaining cumulative gas production, dropout liquid and gas compressibility factor. Data reported from these laboratory experiments are tabulated in Tables 9 and 10, respectively.

5. Results and discussion

To start regression using this brand-new tuning algorithm, besides the experimental data and other fluid properties, a pool of regression parameters must be designated. The trivial parameters which almost always have been considered as regression parameters are plus fraction properties including critical temperature, critical pressure, critical volume, molecular weight, and binary

Table 2
CCE test results for sample MB at 164 °F.

Pressure (psi)	Relative volume
4997	0.9763
4500	0.9795
4000	0.9833
3504	0.9871
3008	0.9913
2810	0.993
2614	0.9948
2514	0.9957
2414	0.9966
2314	0.9976
2214	0.9985
2053	1.0000
2036	1.0023
2023	1.0041
2006	1.0060
1994	1.0080
1983	1.0096
1972	1.0114
1956	1.0141
1927	1.0182
1889	1.0244
1837	1.0335
1764	1.0478
1670	1.0683
1552	1.0995
1407	1.1398
1242	1.2177
1068	1.3241
885	1.4846
711	1.7254
554	2.0854
519	2.1998

Table 3
Differential liberation test results for sample MB.

Pressure (psi)	*Bo* (bbl/STB)	GOR (Scf/STB)	Oil SG	Gas Z factor
4997	1.2723	497.06	0.803	–
4500	1.2765	497.06	0.800	–
4000	1.2814	497.06	0.797	–
3504	1.2864	497.06	0.794	–
3008	1.2918	497.06	0.791	–
2810	1.2941	497.06	0.789	–
2614	1.2964	497.06	0.788	–
2514	1.2976	497.06	0.787	–
2414	1.2988	497.06	0.787	–
2314	1.3001	497.06	0.786	–
2214	1.3013	497.06	0.785	–
2053	1.3032	497.06	0.784	–
1763	1.2830	444.26	0.790	0.858
1513	1.2614	392.68	0.797	0.856
1263	1.2416	343.17	0.803	0.872
1013	1.2213	296.27	0.811	0.887
763	1.2010	249.11	0.818	0.893
513	1.1806	199.25	0.825	0.906
263	1.1571	144.03	0.833	–
14.7	1.0415	0	–	–

SG: Specific gravity, Bo: Oil formation volume factor.

interaction coefficient. Table 11 shows the regression parameters set for tuning of sample MB. Genetic algorithm setting parameters applied for this sample is defined in Table 12. As discussed previously, in non-sorted type of GA, despite conventional method, weight factors are completely eradicated from tuning process and each property is assessed individually to obtain the objective function. The initial datasets defined as initial population are built randomly based on lower and upper bound of regression parameters as tabulated in Table 12. Eventually, as mentioned before, the tuning process continues based on the non-sorted genetic algorithm. The key features which help algorithm to create qualified generations and also avoid it to be trapped in local minimum are crossover and mutation. Although front based ranking operation with crowding distance selection, creates suitable diversity in the solutions, they help to achieve better convergency as well. During the tuning process, it is possible to filter the solution based on the individual relative error percentage for each defined property. The error filter shown in Fig. 4 has been defined arbitrarily for this case based on authors' strategy. Implementing this filter, 9 distinguished solutions, namely MB_0, MB_1, MB_2, MB_3, MB_4, MB_5, MB_6, MB_7, and MB_8 have been defined as the convenient options for fluid sample MB.

Table 4
Fluid composition of sample MI.

Component	Mole percent
N_2	0.002
CO_2	0.007
C_1	0.240
C_2	0.080
C_3	0.055
IC_4	0.010
NC_4	0.030
IC_5	0.012
NC_5	0.015
FC_6	0.052
FC_7	0.032
FC_8	0.031
FC_9	0.032
FC_{10}	0.025
FC_{11}	0.022
C_{12+}	0.354

Table 5
CCE test results for sample MI at 110 °F.

Pressure (psi)	Relative volume
4049	0.991
3045	0.995
2542	0.996
2038	0.997
1836	0.998
1735	0.999
1633	0.999
1533	1.000
1432	1.006
1352	1.009
1324	1.012
1315	1.014
1304	1.017
1293	1.020
1280	1.029
1269	1.039
1234	1.052
1203	1.072
1161	1.102
1103	1.147
1031	1.216
940	1.319
832	1.473
726	1.704
612	2.051
490	2.556
397	3.190

The most prominent fluid property which needs to be reconciled in EOS tuning is saturation pressure which is designated in Table 13. The absolute error percent obtained for this parameter is less than 0.5 compared to the experimental value which is close to 2050 psi determined from manual matching. Other comparisons received from this regression and manual tuning using WinProp software are

Table 6
CCE test results for sample MI at 225°F.

Pressure (psi)	Relative volume
5050	0.970
4049	0.978
3045	0.986
2542	0.991
2340	0.993
2240	0.994
2139	0.995
2038	0.996
1937	0.998
1836	0.999
1739	1.000
1723	1.003
1706	1.006
1694	1.008
1681	1.011
1671	1.013
1661	1.015
1640	1.019
1617	1.025
1581	1.033
1533	1.045
1465	1.064
1376	1.092
1266	1.134
1135	1.197
989	1.293
837	1.436
687	1.652
549	1.975
427	2.460
353	2.928

Table 7
Differential liberation test results for sample MI at 225 °F.

Pressure (psi)	B_o (bbl/STB)	GOR (Scf/STB)	Oil SG	Gas Z Factor	Gas FVF (Scf/ft	Gas SG	Visc. Gas (*Cp*)
5050	1.305	430.1	0.785	–	–	–	–
4049	1.315	430.1	0.779	–	–	–	–
3045	1.326	430.1	0.773	–	–	–	–
2542	1.332	430.1	0.769	–	–	–	–
2340	1.335	430.1	0.768	–	–	–	–
2240	1.336	430.1	0.767	–	–	–	–
2138	1.337	430.1	0.766	–	–	–	–
2038	1.339	430.1	0.765	–	–	–	–
1937	1.340	430.1	0.764	–	–	–	–
1836	1.342	430.1	0.763	–	–	–	–
1737	1.343	430.1	0.763	–	–	–	–
1530	1.326	391.3	0.768	0.879	0.011	0.778	0.016
1230	1.300	333.8	0.775	0.894	0.014	0.799	0.015
925	1.274	276.5	0.783	0.914	0.019	0.815	0.014
622	1.247	216.7	0.791	0.939	0.029	0.854	0.013
319	1.218	150.2	0.799	0.967	0.059	0.971	0.013
14.7	1.064	–	0.865	1.000	–	1.418	0.010

GOR: Gas oil ratio, FVF: Formation volume factor, Visc.: viscosity.

Table 8
Composition of sample MA.

Component	Mole percent
N_2	0.001
CO_2	0.022
CH_4	0.658
C_2H_6	0.056
C_3H_8	0.028
IC_4	0.008
NC_4	0.017
IC_5	0.010
NC_5	0.012
FC_6	0.023
FC_7	0.028
FC_8	0.032
FC_9	0.026
FC_{10}	0.018
FC_{11}	0.012
C_{12}–C_{14}	0.033
C_{15}	0.005
C_{16}–C_{17}	0.006
C_{18+}	0.005

Table 9
CCE test results for sample MA at 304°F.

Pressure	Relative volume
8500	0.8936
8300	0.9030
8100	0.9126
7900	0.9226
7700	0.9328
7500	0.9438
7200	0.9614
6800	0.9871
6620	1.0000
6300	1.0247
6000	1.0508
5600	1.0887
5200	1.1327
4800	1.1864
4400	1.2500
4000	1.3399
3600	1.4665
3200	1.6349
2800	1.8707
2400	2.2412
2000	2.7550
1600	3.5017
1400	4.0749

Table 10
CVD test results for sample MA at 304°F.

Pressure (psi)	Cum. gas prod. (%)	Liquid drop (%)	Gas Z factor
6620	0	0	–
5500	7.780	9.68	1.037
4500	17.74	21.90	0.990
3500	32.02	29.21	0.955
2200	52.26	33.76	0.937
1200	75.20	29.77	0.947

Cum.: cumulative, Prod.: production.

Table 11
Regression parameter set for sample MB.

Variable	Component	Lower bound	Upper bound	Initial value
P_C	FC_6	28.6	32.9	31.9
	C_7–C_{13}	23.2	27.6	27.5
	C_{14}–C_{21}	16.2	23.2	22.6
	C_{22+}	8.24	1.63	8.88
V_C	C_{22+}	1.01	1.52	1.38
	C_{14}–C_{21}	0.637	0.955	0.921
	C_7–C_{13}	0.392	0.588	0.491
	FC_6	0.275	0.413	0.324
T_C	FC_6	490	543	491
	C_7–C_{13}	576	706	693
	C_{14}–C_{21}	621	889	816
	C_{22+}	914	1390	914
AF	FC_6	0.264	0.298	0.272
	C_7–C_{13}	0.319	0.481	0.435
	C_{14}–C_{21}	0.357	0.895	0.894
	C_{22+}	0.946	1.72	0.951
MW	C_{22+}	457	685	473
	C_{14}–C_{21}	179	269	211
	C_7–C_{13}	111	167	165
	FC_6	68.8	103	101
PVC_3		0	1.80	0.871

P_c: critical pressure, V_c: critical volume, T_c: critical temperature, AF: acentric factor, MW: molecular weight, PVC3: hydrocarbon binary interaction exponent, *F*: typical hydrocarbon fraction.

Table 12
Genetic algorithm setting parameters for tuning of samples MB, MI and MA.

GA setting parameter	Value
Population size	50
Crossover rate	0.6
Generation size	100
Mutation rate	0.2

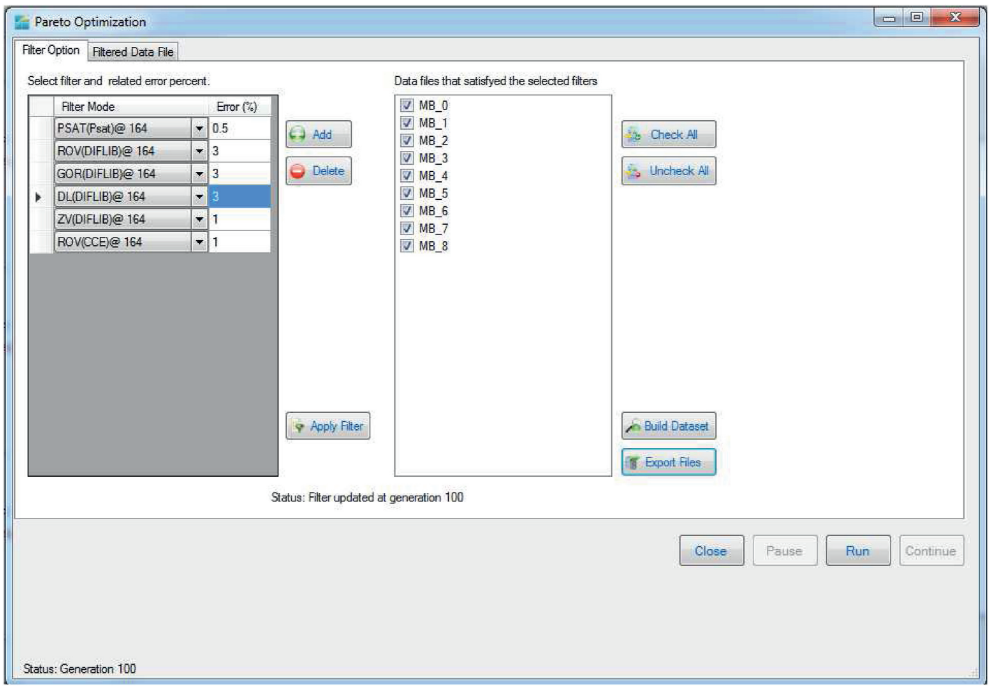

Fig. 4. Maximum error percent selected to filter the best matches for sample MB (acquired from the developed software).

Table 13
Determined saturation pressure for filtered best matches for sample MB at 164°F.

Filtered best model	Experimental Sat. pressure (psi)	Calculated Sat. pressure (psi)	Absolute error (%) Abs (($Psat^{calc}$-$Psat^{Exp}$)*100/$Psat^{Exp}$)
MB_0	2053	2046.8	0.302
MB_1	2053	2044.4	0.419
MB_2	2053	2057.8	0.234
MB_3	2053	2059.7	0.326
MB_4	2053	2045.4	0.370
MB_5	2053	2048.8	0.205
MB_6	2053	2059.2	0.302
MB_7	2053	2052.6	0.019
MB_8	2053	2055.4	0.117

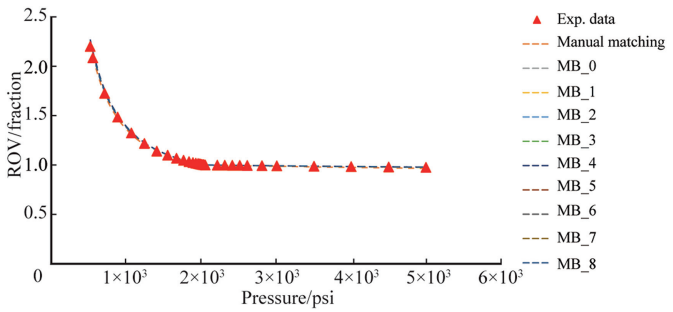

Fig. 5. Comparison of calculated relative oil volume data of sample MB amongst filtered best matches in CCE test at 164°F.

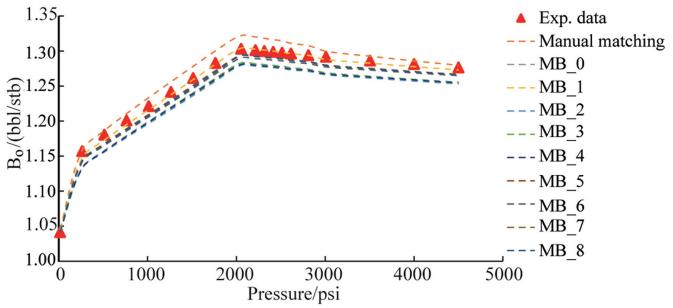

Fig. 6. Comparison of calculated oil formation volume factor data of sample MB amongst filtered best matches in DIFLIB test at 164°F.

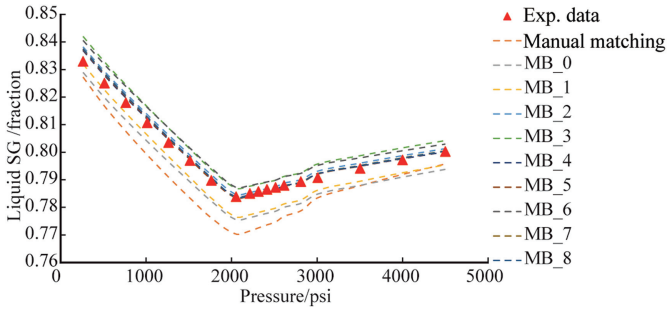

Fig. 7. Comparison of calculated oil density data of Sample MB amongst filtered best matches in DIFLIB test at 164°F.

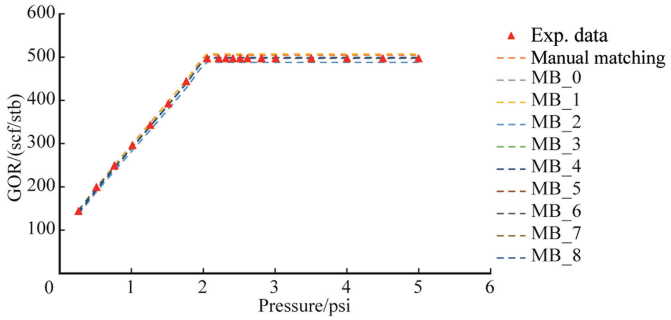

Fig. 8. Comparison of calculated gas oil ratio data of Sample MB amongst filtered best matches in DIFLIB test at 164°F.

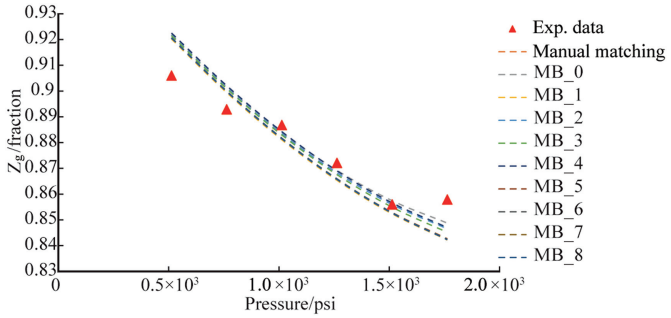

Fig. 9. Comparison of calculated gas compressibility Z factor data of Sample MB amongst filtered best matches in DIFLIB test at 164 °F.

Table 14
Comparison amongst different solutions of sample MB based on minimum, maximum and average error percentage determined at different point pressure for each property (Abs((Prop^{calc}-Prop^{Exp})*100/Prop^{Exp}).

Experimental test		Manual match	MB_0	MB_1	MB_2	MB_3	MB_4	MB_5	MB_6	MB_7	MB_8
ROV(DIFLIB)@ 164	Min error (%)	0.13	0.32	0.02	0.01	0.10	0.12	0.06	0.05	0.07	0.07
	Max error (%)	1.44	2.04	0.80	2.13	2.09	2.09	1.16	1.34	1.22	1.24
	Mean error (%)	0.92	1.65	0.25	1.80	1.61	1.70	0.79	1.02	0.84	0.86
GOR (DIFLIB)@ 164	Min error (%)	0.39	1.87	0.09	1.90	0.12	0.06	0.19	0.25	0.43	0.38
	Max error (%)	1.60	6.04	2.03	4.86	2.74	2.82	1.46	1.49	1.43	1.57
	Mean error (%)	1.24	2.80	1.57	2.70	0.72	0.68	0.45	0.55	0.62	0.63
DL (DIFLIB)@ 164	Min error (%)	0.56	0.48	0.12	0.03	0.33	0.00	0.01	0.34	0.01	0.02
	Max error (%)	1.73	1.11	0.98	0.63	1.09	0.47	0.51	0.91	0.55	0.54
	Mean error (%)	1.30	0.89	0.69	0.23	0.56	0.12	0.15	0.52	0.16	0.16
ZV (DIFLIB)@ 164	Min error (%)	0.09	0.17	0.43	0.01	0.12	0.07	0.37	0.37	0.39	0.40
	Max error (%)	4.06	1.75	1.83	1.72	1.71	1.82	1.78	1.80	1.81	1.82
	Mean error (%)	2.05	0.57	0.88	0.62	0.69	0.60	0.84	0.85	0.86	0.86
ROV(CCE)@ 164	Min error (%)	0.00	0.01	0.01	0.01	0.00	0.00	0.00	0.00	0.00	0.00
	Max error (%)	1.09	2.28	2.50	2.12	3.01	3.20	1.80	2.07	2.05	2.07
	Mean error (%)	0.37	0.35	0.35	0.36	0.41	0.44	0.23	0.32	0.30	0.33

presented in Figs. 5–9 for PVT properties of relative oil volume, oil formation volume factor, oil density, gas-oil ratio, and gas compressibility factor, respectively. Furthermore, some important statistical data such as mean, minimum and maximum error percentages of each property are defined in Table 14 for the aforementioned PVT properties. These comparisons may provide the

Table 15
Regression parameter set for sample MI.

		Lower bound	Upper bound	Initial Value
P_C	FC_{11}	19.8	24.0	21.5
	C_{12+}	12.9	19.5	14.4
T_C	FC_{11}	633	759	703
	C_{12+}	771	1060	821
AF	C_{12+}	0.659	0.987	0.800
MW	C_{12+}	232	348	341
MU	2	0.0187	0.0280	0.0234
	3	0.0468	0.0702	0.0585
	4	−0.0489	−0.0326	−0.04.08
	5	0.00747	0.0112	0.00933
V_cVisc	C_{12+}	0.805	1.21	1.01
OA	C_{12+}	0.366	0.549	0.415
OB	C_{12+}	0.0622	0.0934	0.0853
PVC_3		0.00	1.80	1.10
SH	$C1_{2+}$	−0.153	0.199	0.0154

P_c: critical pressure, T_c: critical temperature, AF: acentric factor, MW: molecular weight, PVC3: hydrocarbon binary interaction exponent, V_cVisc: critical volume related to viscosity correlation, SH: volume shift, MU: coefficient of viscosity correlation, OA: omega A, OB: omega B, *F*: typical hydrocarbon fraction.

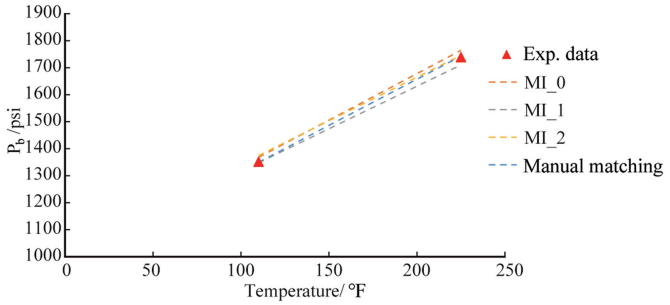

Fig. 10. Comparison of calculated saturation pressure of sample MI amongst filtered best matches in CCE test at different temperature.

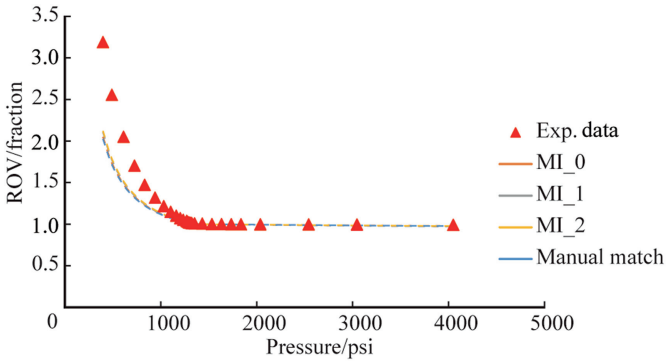

Fig. 11. Comparison of calculated relative total volume of sample MI amongst filtered best matches in CCE test at 110°F.

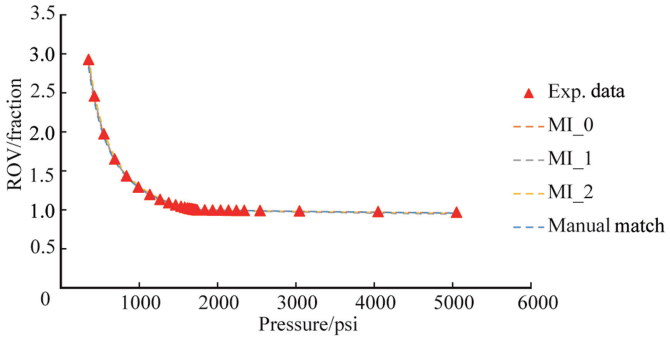

Fig. 12. Comparison of calculated relative total volume of sample MI amongst filtered best matches in CCE test at 225°F.

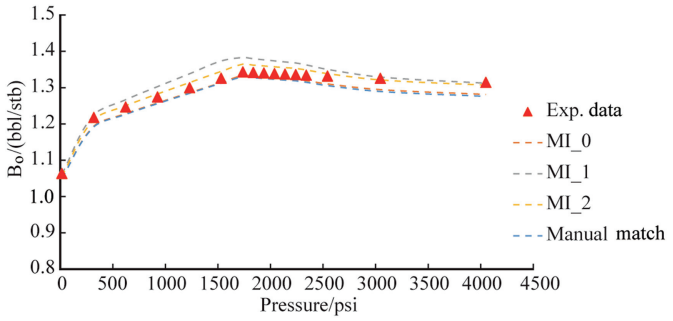

Fig. 13. Comparison of calculated oil formation volume factor data of sample MI amongst filtered best matches in DIFLIB test at 225°F.

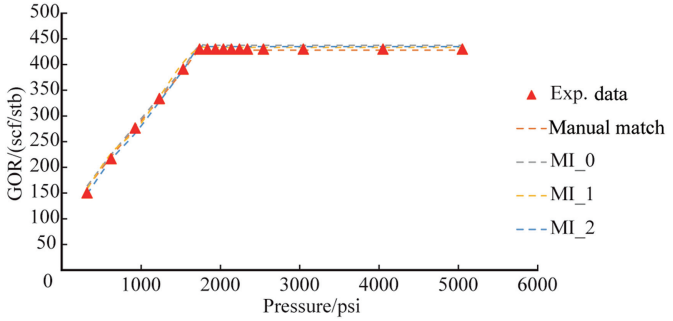

Fig. 14. Comparison of calculated gas oil ratio data of sample MI amongst filtered best matches in DIFLIB test at 225°F.

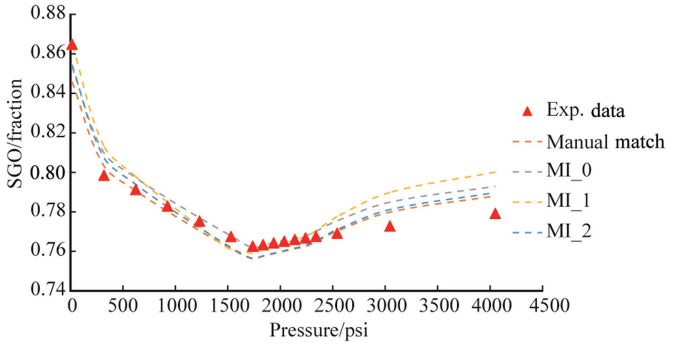

Fig. 15. Comparison of calculated oil specific gravity data of sample MI amongst filtered best matches in DIFLIB test at 225°F.

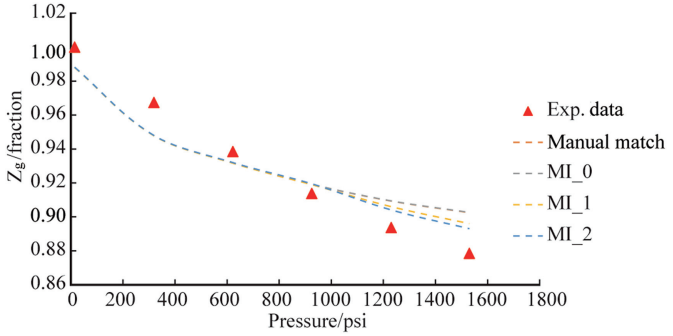

Fig. 16. Comparison of calculated gas compressibility z factor data of sample MI amongst filtered best matches in DIFLIB test at 225°F.

experts with multi solutions to the problem at hand and help them to manipulate amongst choices they may need for future assessment.

To investigate the capability of algorithm on experimental data at a different test temperature, another black oil fluid sample, namely MI was examinated. Table 15 shows the regression parameter set for tuning of this sample. GA setting parameters tabulated in Table 12 are applied here as well. Similarly, such as the previous problem, one can choose amongst final solution based on his/her own strategy. Based on the maximum user-entered error after the end of regression process, three convenient options including MI_0, MI_1 and MI_2 were defined for this sample. Results shown in Fig. 10 represent bubble point

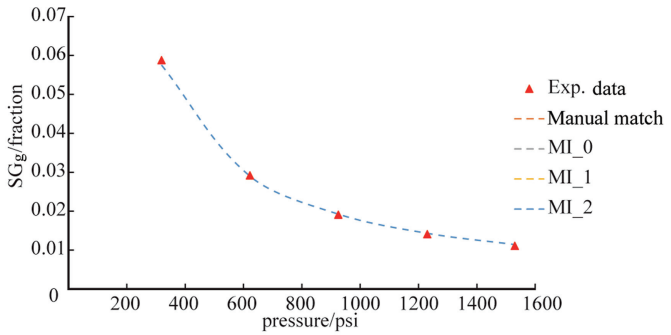

Fig. 17. Comparison of calculated gas specific gravity data of sample MI amongst filtered best matches in DIFLIB test at 225°F.

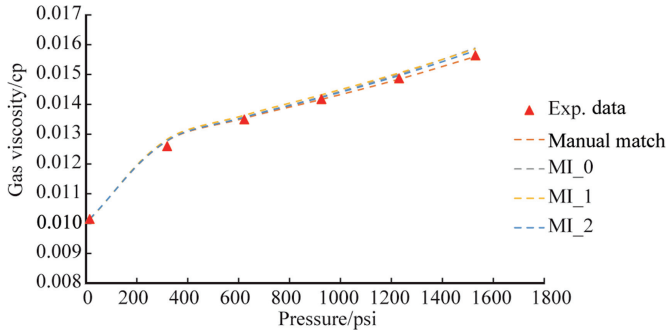

Fig. 18. Comparison of calculated gas viscosity data of sample MI amongst filtered best matches in DIFLIB test at 225°F.

Table 16
Comparison amongst different solutions of sample MI based on minimum, maximum and average error percentage determined at different point pressure for each property (Abs((Prop^{calc}-Prop^{Exp})*100/Prop^{Exp}).

Experimental test		Manual match	MI_0	MI_1	MI_2
ROV (CCE) @ 110°F	Min error (%)	0.20	0.17	0.26	0.02
	Max error (%)	28.41	27.74	26.62	26.08
	Mean error (%)	4.74	4.41	4.52	4.05
ROV (CCE) @ 225°F	Min error (%)	0.00	0.01	0.06	0.05
	Max error (%)	3.25	1.87	2.61	1.99
	Mean error (%)	0.51	0.54	0.86	0.73
GOR (DIFLIB) @ 225°F	Min error (%)	0.06	0.44	0.73	0.42
	Max error (%)	6.73	8.92	5.16	3.76
	Mean error (%)	0.94	2.17	1.49	1.30
BO (DIFLIB) @ 225°F	Min error (%)	1.02	0.72	0.16	0.29
	Max error (%)	2.94	2.54	3.57	1.59
	Mean error (%)	1.55	1.30	1.94	0.98
SGO (DIFLIB) @225°F	Min error (%)	0.07	0.01	0.02	0.04
	Max error (%)	2.20	1.76	2.68	1.35
	Mean error (%)	0.71	0.58	0.73	0.67
ZV (DIFLIB) @ 225°F	Min error (%)	0.59	0.59	0.57	0.62
	Max error (%)	2.73	2.75	2.03	2.01
	Mean error (%)	1.50	1.50	1.32	1.22
BG (DIFLIB) @ 225°F	Min error (%)	0.67	0.66	0.68	0.65
	Max error (%)	2.89	2.91	2.86	2.95
	Mean error (%)	1.59	1.60	1.58	1.62
SGV (DIFLIB) @ 225°F	Min error (%)	1.42	1.48	1.03	1.56
	Max error (%)	3.91	3.98	3.56	4.08
	Mean error (%)	2.64	2.71	2.27	2.80
Gas Viscosity (DIFLIB) @ 225°F	Min error (%)	0.02	0.04	0.13	0.03
	Max error (%)	1.40	1.60	1.82	1.48
	Mean error (%)	0.37	0.87	1.11	0.68

pressure at different temperatures of 110°F and 120°F for manual and automated matching method compared to experimental results. Other comparisons for CCE and DIFLIB (differential liberation) data adjustment are presented in Figs. 11–18 for relative total volume at 110°F, relative total volume, oil formation volume factor, gas-oil ratio, oil specific gravity, gas compressibility factor, gas specific data, and gas viscosity data all at 225°F. To have better assessment of algorithm capability and validate the attained solutions, common statistical data shown in Table 16 may be used.

In addition to the above samples MB and MI, a more complex gas condensate fluid sample (sample MA) was designated to verify the

Table 17
Regression parameter set for sample MA.

		Lower bound	Upper bound	Initial Value
P_C	C_{12}–C_{14}	2.02×10^{1}	2.25×10^{1}	2.06×10^{1}
	C_{15}	1.79×10^{1}	1.95×10^{1}	1.91×10^{1}
	C_{16}–C_{17}	1.63×10^{1}	1.79×10^{1}	1.64×10^{1}
	C_{18+}	1.21×10^{1}	1.82×10^{1}	1.64×10^{1}
T_C	C_{12}–C_{14}	6.66×10^{2}	7.05×10^{2}	6.93×10^{2}
	C_{15}	7.07×10^{2}	7.36×10^{2}	7.36×10^{2}
	C_{16}–C_{17}	7.37×10^{2}	7.72×10^{2}	7.51×10^{2}
	C_{18+}	6.40×10^{2}	9.60×10^{2}	7.33×10^{2}
AF	C_{12}–C_{14}	$4.85\times10\text{-}^{1}$	5.27×10^{-1}	5.18×10^{-1}
	C_{15}	5.18×10^{-1}	5.91×10^{-1}	5.50×10^{-1}
	C_{16}–C_{17}	5.91×10^{-1}	6.68×10^{-1}	6.14×10^{-1}
	C_{18+}	5.83×10^{-1}	8.75×10^{-1}	7.90×10^{-1}
MW	C_{12}–C_{14}	1.42×10^{2}	2.12×10^{2}	1.54×10^{2}
	C_{15}	1.67×10^{2}	2.50×10^{2}	2.37×10^{2}
	C_{16}–C_{17}	1.83×10^{2}	2.74×10^{2}	1.83×10^{2}
	C_{18+}	2.25×10^{2}	3.38×10^{2}	3.38×10^{2}
SH	C_{12}–C_{14}	1.15×10^{-1}	2.15×10^{-1}	2.01×10^{-1}
	C_{15}	-1.79×10^{-2}	1.82×10^{-1}	1.82×10^{-1}
	C_{16}–C_{17}	-1.00×10^{-2}	1.90×10^{-1}	1.77×10^{-1}
	C_{18+}	5.40×10^{-2}	1.54×10^{-1}	6.82×10^{-2}
OA	C_{12}–C_{14}	3.66×10^{-1}	5.49×10^{-1}	4.51×10^{-1}
	C_{15}	3.66×10^{-1}	5.49×10^{-1}	3.90×10^{-1}
	C_{16}–C_{17}	2.93×10^{-1}	4.39×10^{-1}	4.19×10^{-1}
	C_{18+}	3.66×10^{-1}	5.49×10^{-1}	3.66×10^{-1}
OB	C_{12}–C_{14}	6.22×10^{-2}	9.34×10^{-2}	6.42×10^{-2}
	C_{15}	7.47×10^{-2}	1.12×10^{-1}	8.91×10^{-2}
	C_{16}–C_{17}	7.47×10^{-2}	1.12×10^{-1}	1.02×10^{-1}
	C_{18+}	6.22×10^{-2}	9.34×10^{-2}	6.52×10^{-2}

P_c: critical pressure, T_c: critical temperature, AF: acentric factor, MW: molecular weight.
SH: volume shift, OA: omega A, OB: omega B.

Table 18
Determined saturation pressure for filtered best matches of sample MA.

Filtered best model	Experimental Sat. pressure (psi)	Calculated Sat. pressure (psi)	Absolute relative error (%)
MA_0	6620	6609.5	0.16
MA_1	6620	6658.3	0.58
MA_2	6620	6656.9	0.56
MA_3	6620	6674.6	0.82

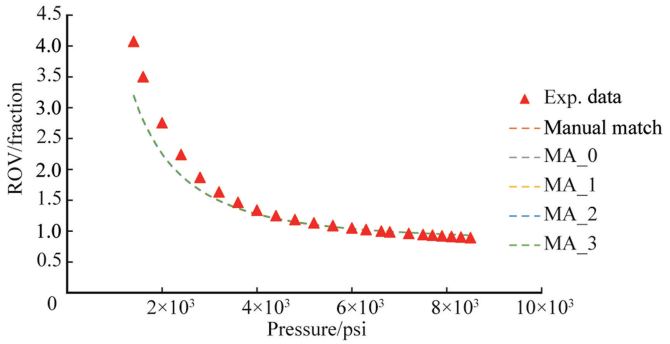

Fig. 19. Comparison of calculated relative oil volume data of sample MA amongst filtered best matches in CCE test at 304°F.

capability of this sophisticated tuning algorithm. Table 17 shows the regression parameter set for tuning this sample. GA setting parameters tabulated in Table 12 are applied here as well. Based on authors' strategy, four distinguished solutions have been defined, including MA_0, MA_1, MA_2, and MA_3, from which, similar to previous samples, one can choose amongest final solution based on his/her own strategy.

Dew point pressure which is precedent to other properties is defined in Table 18. The absolute error obtained is less than 1% which shows the good accuracy of this algorithm. Other comparisons received from this regression are displayed in Figs. 19–22 for relative oil volume, cumulative gas production, liquid dropout, and gas compressibility factor, respectively. These solutions refer to kind of solutions which are non-dominated to each other, while being superior to other solutions. To have better comparison, other statistical data which are defined in Table 19, may be used for foregoing analysis.

The statistical data (error values) for the aforementioned three PVT samples show that all the solutions using the employed algorithm and the obtained solution via manual tuning process are trustworthy. The manual PVT tuning approach has been used worldwide, however, with the main drawback being almost always time-consuming. In fact, depending on the complexity of fluid model, the manual tuning process might take multiple weeks and become an arduous task. As it is completely

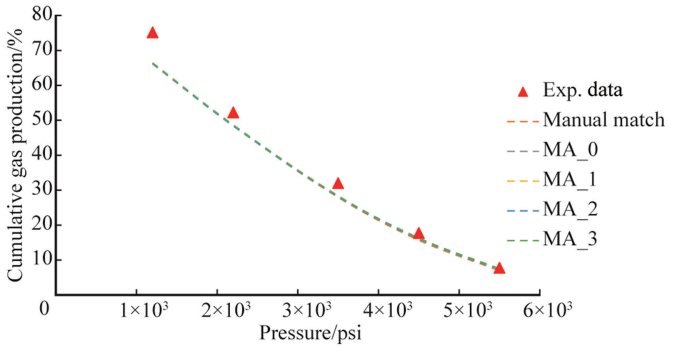

Fig. 20. Comparison of calculated cumulative gas production data of sample MA amongst filtered best matches in CVD test at 304°F.

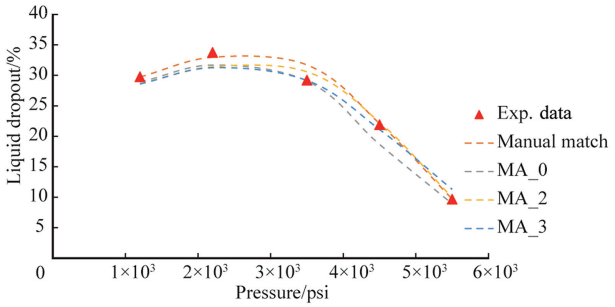

Fig. 21. Comparison of calculated liquid dropout data of sample MA amongst filtered best matches in CVD test at 304°F.

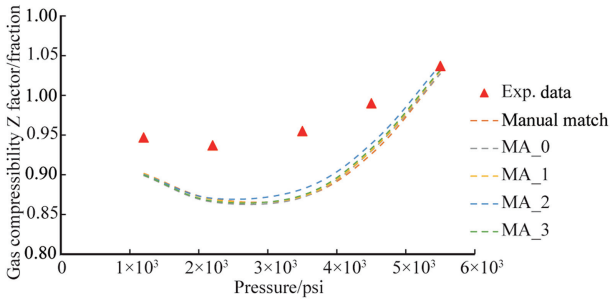

Fig. 22. Comparison of calculated gas compressibility factor data of sample MA amongst filtered best matches in CVD test at 304°F.

Table 19
Comparison amongst different solutions of Sample MA based on minimum, maximum and average error percentage determined at different point pressure for each property ($Abs((Prop^{calc}-Prop^{Exp})*100/Prop^{Exp})$).

Experimental Test		Manual Match	MB_0	MB_1	MB_2	MB_3
MV (CVD) @ 304	Min error (%)	7.35	6.99	5.57	6.70	3.49
	Max error (%)	12.64	11.97	11.78	12.04	11.70
	Mean error (%)	10.85	9.43	9.11	9.55	8.32
VL (CVD) @ 304	Min error (%)	0.14	3.36	0.48	1.83	0.14
	Max error (%)	8.57	11.99	14.73	6.96	16.73
	Mean error (%)	2.44	7.86	6.39	4.04	6.37
ZV (CVD) @ 304	Min error (%)	0.94	0.93	0.61	0.13	0.51
	Max error (%)	8.69	8.74	8.61	7.64	8.46
	Mean error (%)	5.61	5.68	5.46	4.99	5.44
ROV (CCE) @ 304	Min error (%)	0.02	0.05	0.21	0.20	0.28
	Max error (%)	21.64	21.31	21.29	21.75	21.35
	Mean error (%)	6.23	6.01	6.06	6.15	6.03

evident from above results, using Pareto front based evolutionary algorithm facilitates the tuning process even in complex PVT fluid models and statistical data clearly depict that this new algorithm has been more precise and vigorous than common conventional procedure.

6. Conclusions

In this work, the application of a multi-objective optimization algorithm, namely NSGA-II was introduced for the purpose of auto-tuning PVT data. For this purpose, and to imply the

comprehensiveness of presented method, three different fluid samples (two black-oil and one gas condensate sample) which are different in PVT properties and experimental data, were taken into account. The statistical error data demonstrated that the proposed auto-tuning method is accurate and robust. In contrast to the manual matching process, the aforementioned technique is fast, and may provide the engineer with several solutions from which one solution can be selected based upon the engineering background and circumstances at hand. Moreover, using the applied methodology, one is not compelled to concern themselves with choosing the tuning parameters, and additionally weight factors with some level of uncertainty, which are the essential part of the manual tuning approach as arduous and time-consuming tasks.

Declaration of competing interest

The authors declare that they have no known competing financial interests or personal relationships that could have appeared to influence the work reported in this paper.

References

[1] A. Kumar, R. Okuno, Characterization of reservoir fluids using an EoS based on perturbation from n-alkanes, Fluid Phase Equil. 358 (2013) 250–271.
[2] A. Daryasafar, M. Masoudi, S. Kord, M. Madani, Evaluation of different thermodynamic models in predicting asphaltene precipitation: a comparative study, Fluid Phase Equil. 514 (2020) 112557.
[3] R.A. Almehaideb, A.S. Al-Khanbashi, M. Abdulkarim, M.A. Ali, EOS tuning to model full field crude oil properties using multiple well fluid PVT analysis, J. Petrol. Sci. Eng. 26 (1–4) (2000) 291–300.
[4] I. Ashour, N. Al-Rawahi, A. Fatemi, G. Vakili-Nezhaad, Applications of equations of state in the oil and gas industry, Therm. Kinet. Dyn. Syst. 7 (2011) 165–178.
[5] T.O. Amao, A.M. Amao, Fluid Characterization and EoS Modelling of PVT Experiments. *SPE Nigeria Annual International Conference And Exhibition*, Society of Petroleum Engineers, 2014.
[6] R. Nazemi, A. Daryasafar, A. Bazyari, S.A. Shafiee Najafi, S. Ashoori, Modeling asphaltene precipitation in live crude oil using cubic plus association (CPA) equation of state, Petrol. Sci. Technol. 38 (3) (2020) 257–265.
[7] A. Daryasafar, A. Ahadi, R. Kharrat, Modeling of steam distillation mechanism during steam injection process using artificial intelligence, Sci. World J. 2014 (2014).
[8] A. Zarifi, A. Daryasafar, Auto-tune of PVT data using an efficient engineering method: application of sensitivity and optimization analyses, Fluid Phase Equil. 473 (2018) 70–79.
[9] O. Redlich, J.N. Kwong, On the thermodynamics of solutions. V. An equation of state. Fugacities of gaseous solutions, Chem. Rev. 44 (1) (1949) 233–244.
[10] G. Soave, Equilibrium constants from a modified Redlich-Kwong equation of state, Chem. Eng. Sci. 27 (6) (1972) 1197–1203.
[11] D.-Y. Peng, D.B. Robinson, A new two-constant equation of state, Ind. Eng. Chem. Fundam. 15 (1) (1976) 59–64.
[12] A. Daryasafar, A. Soleymanzadeh, K. Shahbazi, A New Generalized Auto-Tune Procedure for Modeling Asphaltene Precipitation by Equation of State 82nd EAGE Annual Conference & Exhibition, European Association of Geoscientists & Engineers, 2021, pp. 1–5, 2021.
[13] M.T. Sarvestani, B.S. Sola, F. Rashidi, Genetic algorithm application for matching ordinary black oil PVT data, Petrol. Sci. 9 (2) (2012) 199–211.
[14] S. Leekumjorn, K. Krejbjerg, Phase behavior of reservoir fluids: comparisons of PC-SAFT and cubic EOS simulations, Fluid Phase Equil. 359 (2013) 17–23.
[15] W. Yan, F. Varzandeh, E.H. Stenby, PVT modeling of reservoir fluids using PC-SAFT EoS and Soave-BWR EoS, Fluid Phase Equil. 386 (2015) 96–124.
[16] F. Varzandeh, E.H. Stenby, W. Yan, General approach to characterizing reservoir fluids for EoS models using a large PVT database, Fluid Phase Equil. 433 (2017) 97–111.
[17] Y. Khoshnamvand, M. Assareh, B.M. Davoudi, Phase behavior modeling for gas condensate fluids with PC-SAFT and an improved binary interaction coefficient model, Fluid Phase Equil. 444 (2017) 37–46.
[18] K. Coats, G. Smart, Application of a regression-based EOS PVT program to laboratory data, SPE Reservoir Eng. 1 (3) (1986) 277–299.
[19] P. Christensen, Regression to experimental PVT data, J. Can. Petrol. Technol. 38 (13) (1999).
[20] C.H. Whitson, M.R. Brulé, Phase Behavior, Henry L. Doherty Memorial Fund of AIME, Society of Petroleum Engineers, 2000.
[21] M. Gen, R. Cheng, L. Lin, Network Models and Optimization: Multiobjective Genetic Algorithm Approach, Springer Science & Business Media, 2008.
[22] M. Mitchell, An Introduction to Genetic Algorithms, MIT press, 1998.
[23] P. Poon, G.T. Parks, Optimising PWR Reload Cores, 1992.
[24] J. Grefenstette, R. Gopal, B. Rosmaita, D. Van Gucht, Genetic Algorithms for the Traveling Salesman Problem, in: Proceedings of the First International Conference on Genetic Algorithms and Their Applications 160, Lawrence Erlbaum, 1985, pp. 160–168.
[25] I.C. Parmee, A.H. Watson, Preliminary airframe design using co-evolutionary multiobjective genetic algorithms, in: Proceedings of the 1st Annual Conference on Genetic and Evolutionary Computation 2, 1999, pp. 1657–1665.
[26] M. Madani, M.K. Moraveji, M. Sharifi, Modeling apparent viscosity of waxy crude oils doped with polymeric wax inhibitors, J. Petrol. Sci. Eng. 196 (2021) 108076.
[27] A.B. Shoushtari, S.R. Asadolahpour, M. Madani, Thermodynamic investigation of asphaltene precipitation and deposition profile in wellbore: a case study, J. Mol. Liq. 320 (2020) 114468.
[28] C. Romero, J. Carter, Using genetic algorithms for reservoir characterisation, J. Petrol. Sci. Eng. 31 (2–4) (2001) 113–123.
[29] O. Velez-Langs, Genetic algorithms in oil industry: an overview, J. Petrol. Sci. Eng. 47 (1–2) (2005) 15–22.
[30] C. Coello, A.D. Christiansen, Multiobjective optimization of trusses using genetic algorithms, Comput. Struct. 75 (6) (2000) 647–660.
[31] A. Osyczka, Multicriteria Optimization for Engineering Design. Design Optimization, Elsevier, 1985, pp. 193–227.
[32] C.M. Fonseca, P.J. Fleming, Genetic Algorithms for Multiobjective Optimization: FormulationDiscussion and Generalization. Icga 93, Citeseer, 1993, pp. 416–423.
[33] C.A.C. Coello, G.B. Lamont, D.A. Van Veldhuizen, Evolutionary Algorithms for Solving Multi-Objective Problems, Springer, 2007.
[34] V. Pareto, Cours D'économie Politique, Rouge. Lausanne, Switzerland, 1896.
[35] D.E. Goldberg, Genetic Algorithms in Search. Optimization, and Machine-Learning, 1989.
[36] A. Toffolo, E. Benini, Genetic diversity as an objective in multi-objective evolutionary algorithms, Evol. Comput. 11 (2) (2003) 151–167.
[37] M.M. Etghani, M.H. Shojaeefard, A. Khalkhali, M. Akbari, A hybrid method of modified NSGA-II and TOPSIS to optimize performance and emissions of a diesel engine using biodiesel, Appl. Therm. Eng. 59 (1–2) (2013) 309–315.
[38] J. Yazdi, A. Sadollah, E. Lee, D. Yoo, J.H. Kim, Application of multi-objective evolutionary algorithms for the rehabilitation of storm sewer pipe networks, J. Flood Risk Manag. 10 (3) (2017) 326–338.
[39] K. Deb, A. Pratap, S. Agarwal, T. Meyarivan, A fast and elitist multiobjective genetic algorithm: NSGA-II, IEEE Trans. Evol. Comput. 6 (2) (2002) 182–197.
[40] A. Singh, S. Parida, A multiple strategic evaluation for fault detection in electrical power system, Int. J. Electr. Power Energy Syst. 48 (2013) 21–30.
[41] M.B. Shadmand, R.S. Balog, Multi-objective optimization and design of photovoltaic-wind hybrid system for community smart DC microgrid, IEEE Trans. Smart Grid 5 (5) (2014) 2635–2643.
[42] S. Wang, D. Zhao, J. Yuan, H. Li, Y. Gao, Application of NSGA-II Algorithm for fault diagnosis in power system, Elec. Power Syst. Res. 175 (2019) 105893.
[43] K. Deb, S. Agrawal, A. Pratap, T. Meyarivan, A Fast Elitist Non-dominated Sorting Genetic Algorithm for Multi-Objective Optimization: NSGA-II, in: International Conference on Parallel Problem Solving from Nature, Springer, 2000, pp. 849–858.
[44] K. Deb, Multi-objective Optimization Using Evolutionary Algorithms, John Wiley & Sons, 2001.
[45] S. Ramesh, S. Kannan, S. Baskar, Application of modified NSGA-II algorithm to multi-objective reactive power planning, Appl. Soft Comput. 12 (2) (2012) 741–753.
[46] W. module Tutorial, Computer Modeling Group, Version, 2020.